engineering proceedings

MDPI

Proceeding Paper

Instance Segmentation based Automated Detection and Thickness Estimation of Oil Spills in Aerial Imagery †

Timothy Malche [1,*], Priti Maheshwary [2] and Sumegh Tharewal [3]

[1] Department of Computer Applications, Manipal University Jaipur, Jaipur 303007, Rajasthan, India
[2] Department of Computer Science & Engineering, Rabindranath Tagore University, Bhopal 464993, Madhya Pradesh, India; pritimaheshwary@gmail.com
[3] School of Advance Computing, DBS Global University, Dehradun, Uttarakhand, India; sumegh tharewal@gmail.com
* Correspondence: timothy.malche@jaipur.manipal.edu;
† Presented at The 11th International Electronic Conference on Sensors and Applications (ECSA-11), 26–28 November 2024; Available online: https://sciforum.net/event/ecsa-11.

Abstract: An oil spill at sea represents a catastrophic environmental event resulting from the release of oil into marine ecosystems. These incidents pose substantial risks to marine biodiversity, wildlife habitats, and coastal populations, often engendering enduring and widespread repercussions. Cleaning up oil spills is costly due to logistical challenges. Accurate measurement of spill characteristics like volume, thickness, and area of spill is crucial before deploying clean-up crews to optimize resource allocation and reduce expenses. The main objective of this research is to use computer vision to detect oil spills and estimate its thickness, helping in decision-making processes to clean up the spill area. The system architecture proposed in this study integrates a drone equipped with a camera module to inspect sea areas and capture images. These images are processed using a deployed computer vision segmentation model to detect oil spills and estimate oil thickness. Predicted results help in decision-making via a dedicated application by applying predefined criteria to determine the thickness of the spill which further help in taking actions for removal of oil spills. The computer vision model developed in this research could detect and estimate oil thickness with mAP of 91%. The proposed system in this study uses instance segmentation to detect and segment oil spills in drone footage. This computer vision-based approach accurately identifies and outlines oil spill areas, aiding in the selection of efficient cleanup strategies. Real-time monitoring and assessment capabilities enable quick decision-making and effective response measures.

Keywords: Internet of Things; instance segmentation; camera sensor node; computer vision; remote monitoring

Citation: Malche, T.; Maheshwary, P.; Tharewal, S. Instance Segmentation based Automated Detection and Thickness Estimation of Oil Spills in Aerial Imagery. *Eng. Proc.* **2024**, *6*, x. https://doi.org/10.3390/xxxxx

Academic Editor(s):

Published: 26 November 2024

1. Introduction

An oil spill in the sea occurs when liquid petroleum (crude oil, refined oil products, or by-products) is accidentally released into the marine environment. This can happen due to various reasons, including tanker accidents, pipeline leaks, offshore drilling incidents, or operational discharges from ships.

Following are the causes [1] of oil spill in a sea:

- Structural failures, groundings, or collisions of oil tankers can lead to massive oil spills.
- Corrosion, maintenance failures, or natural disasters can cause underwater or onshore pipelines to rupture, releasing oil into the sea.
- Ships discharging oily waste or ballast water improperly can cause localized spills.
- Blowouts or equipment failures during oil extraction can result in large-scale spills.

Oil spills have severe environmental impacts, starting with marine life, as oil coats the fur and feathers of animals like birds and otters, reducing their insulation and buoyancy, often leading to hypothermia or drowning. Ingested oil is toxic, affecting the digestive and reproductive systems of marine organisms. Entire ecosystems, including coral reefs, mangroves, and coastal wetlands, can be devastated by oil spills, disrupting food chains and leading to species decline. The spread of oil on water surfaces creates a spill that blocks sunlight, disrupting photosynthesis in aquatic plants and phytoplankton, which harms fish and other marine life by reducing oxygen levels. Economically, oil spills impact industries such as fishing, tourism, and shipping, causing significant financial losses and necessitating expensive cleanup efforts. Human health is also at risk, with exposure to oil and its fumes causing respiratory issues, skin irritation, and other health problems. The long-term effects of oil spills include persistent environmental contamination, genetic damage to marine species, and prolonged economic recovery for affected communities [2][3].

Continuous environmental monitoring of vulnerable marine areas is crucial for the early detection of oil spill, enabling rapid response to prevent widespread contamination and protect marine ecosystems. This is where the proposed system helps in preventing harms in marine ecosystems due to oil spills. The system architecture for oil spill detection is illustrated in the Figure 1 below. The system involves a drone equipped with a camera module to capture images of sea areas. These images are processed by a deployed model to detect oil spill, and the predictions are used by a decision-making app to assess the spill's severity and guide appropriate response actions.

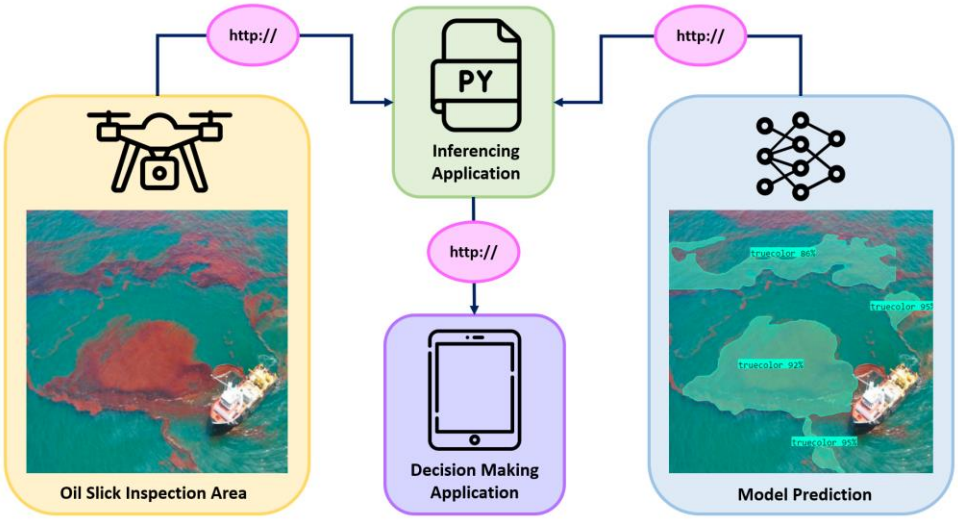

Figure 1. System Architecture.

2. Related Work

Research in [4] provides comprehensive analysis of oil spill distribution and its impact on shoreline ecosystems, identifying key hotspots and contamination risks. The study demonstrates the value of remote sensing data in monitoring and assessing environmental threats in sensitive areas. In [5] authors effectively demonstrate the capability of Sentinel-1 and 2 sensors, along with advanced image processing methods, to detect, monitor, and assess the impact of the Wakashio oil spill on the coastal environment. The research in [6] successfully identifies and analyzes oil spills around the Oil Rocks using multi-temporal ENVISAT radar images. The study in [7] introduces a deep-learning-based method using attention gates in a U-Net architecture to enhance oil spill detection from Sentinel-1 Pol-SAR satellite images. Authors in [8] introduces an innovative framework for detecting oil spills in port environments using UAVs and thermal infrared cameras. By combining automatic annotation of RGB and IR images with convolutional neural network training, the

study achieves an impressive 89% accuracy in real-time oil spill detection. Other past studies [9][10] provides method for oil spill detection using SAR images.

In [11] authors developed a framework for detecting oil spills in port environments using images from UAVs and thermal infrared cameras, with a focus on nighttime detection. The framework includes a training phase to create a dataset by matching RGB and IR images, followed by testing various CNN architectures. The operational phase involves real-time detection with an accuracy of 89%, demonstrated in a controlled experiment in Antwerp. Another study in [12] explores the use of near infrared and shortwave infrared wavelengths to monitoring oil spills. A physical model was developed for accurate oil thickness and volume estimation, and an artificial neural network was used for spill detection. The method was validated in both laboratory and outdoor environments, including drone-mounted RGB camera monitoring of oil spills.

The previous studies demonstrate advancements in oil spill detection using various remote sensing technologies, including SAR, Sentinel-1/2, and UAV-mounted thermal cameras, with significant improvements in accuracy through deep learning and optical reflectance models. These studies highlight the effectiveness of these methods in different environments, from offshore areas to port settings, for monitoring and assessing oil spills. Our study, focused on instance-based segmentation for detecting oil spills, provides more precise identification and segmentation of individual oil spill instances and its class, particularly in complex environments. This approach can enhance the accuracy and reliability of spill detection, enabling better monitoring, targeted cleanup efforts, and reducing false positives compared to traditional methods.

3. Materials & Methods

Cleaning up an oil spill is a costly and challenging process, largely due to the logistical difficulties of accessing affected areas. To optimize resources and reduce expenses, it is crucial to accurately assess the spill's characteristics, such as its volume, thickness, and extent, before deploying a cleanup crew. This precise measurement allows for better planning and more efficient use of resources during the cleanup operation.

Obtaining high resolution aerial images or videos of an oil spill can be analyzed with computer vision models to ensure precise measurement of the spill's dimensions as well as its thickness. This data is crucial for experts in selecting the most effective cleanup method tailored to the spill's characteristics.

For instance, if the oil spill is thin and widely spread, mechanical methods like deploying booms and skimmers may be adequate. However, if the oil spill is thicker or covers a larger area, techniques such as burning or applying chemical dispersants might be more suitable. The coloration of an oil spill on water is influenced by multiple factors, including reflections at the oil-air and oil-water interfaces, as well as internal processes within the oil film itself [13,14]. These phenomena are depicted in Figure 2 [15].

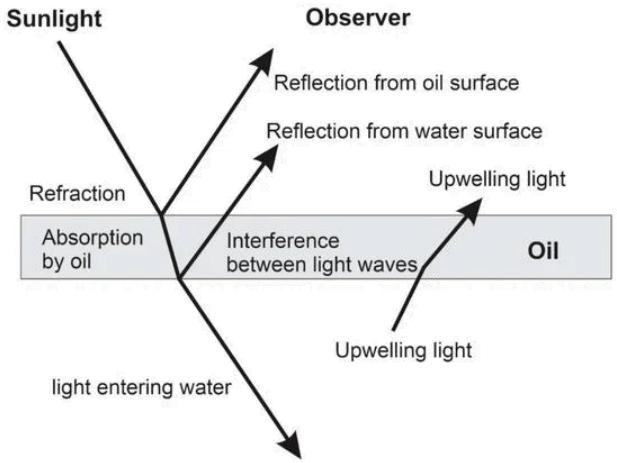

Figure 2. Physics of Oil Spill.

This study focuses on detecting the thickness of an oil spill using computer vision techniques. The estimation of thickness will be derived from the visual characteristics of the oil [16] on the water's surface, particularly the color variations [17–19]. The Figure 3 [20] below presents an aerial view of the oil spill, highlighting the different color codes associated with varying thickness levels.

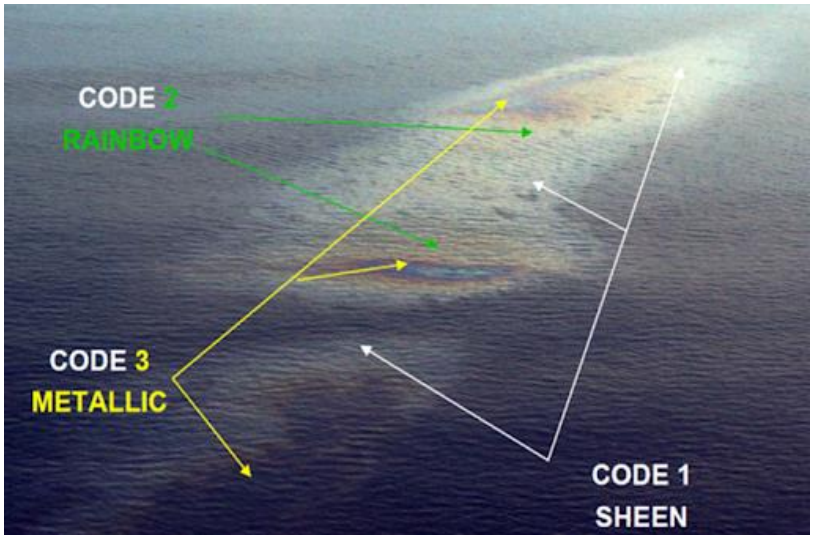

Figure 3. Sample aerial view of Bonn agreement oil spill thickness codes.

This project utilizes image segmentation, specifically instance segmentation, to detect the thickness of oil. The dataset is labeled using three distinct classes (i.e., "rainbow", "sheen", "truecolor") to identify oil spill thickness on water surface. The Figure 4 shows how these classes of oil spill can be seen on water surface. The composition of an oil spill dataset is summarized in Table 1 representing the different subsets used for training, validating, and testing a machine learning model.

(**a**) (**b**) (**c**)

Figure 4. Dataset (**a**) Rainbow, (**b**) Sheen, (**c**) True Color.

Table 1. Oil Spill Dataset.

		Training	Validation	Testing
Total	1475	886	295	294
Rainbow	478	287	96	95
Sheen	501	301	100	100
True Color	496	298	99	99

The dataset is labeled to classify each of these classes for the instance segmentation model. The dataset is labeled using the polygon bounding boxes covering the oil spill area in the image as shown in the Figure 5 below.

(**a**) (**b**) (**c**)

Figure 5. Class Labels (**a**) Rainbow, (**b**) Sheen, (**c**) True Color.

4. Results and Discussion

The instance segmentation model has been trained using the YOLOv8 pretrained Segment models which are trained on COCO dataset [21].

Following (in Table 2) are the latest releases of pre-trained YOLOv8 segmentation models by Ultralytics [22]. These different models are experimented in this research and finally the model trained with YOLOv8m-seg has been selected. This model does not only offer accuracy but also latency.

Table 2. Pretrained YOLOv8 segmentation models.

Model	Size (Pixels)	mAP (Box) 50–95	mAP (Mask) 50-95
YOLOv8n-seg	640	36.7	30.5
YOLOv8s-seg	640	44.6	36.8
YOLOv8m-seg	640	49.9	40.8
YOLOv8l-seg	640	52.3	42.6
YOLOv8x-seg	640	53.4	43.4

Training the YOLOv8m-seg model on the custom oil spill dataset, the mAP of 91% has been achieved. The following Table 3 illustrates that the trained model performs well for both bounding box and mask detection for overall category as well as class wise categories.

Table 3. Performance metrics of segmentation model.

	Box			Mask		
	P	**R**	**mAP50**	**P**	**R**	**mAP50**
All	0.909	0.952	0.913	0.915	0.935	0.912
Rainbow	0.986	1	0.995	0.986	1	0.995
Sheen	0.831	0.874	0.818	0.85	0.821	0.813
True Color	0.91	0.984	0.927	0.91	0.984	0.929

The images in Figure 6 below demonstrate that the model performs well on test images. The model segment each oil spill with good accuracy and can even segment multiple classes in the same images. This helps to identify the thickness of oil spill.

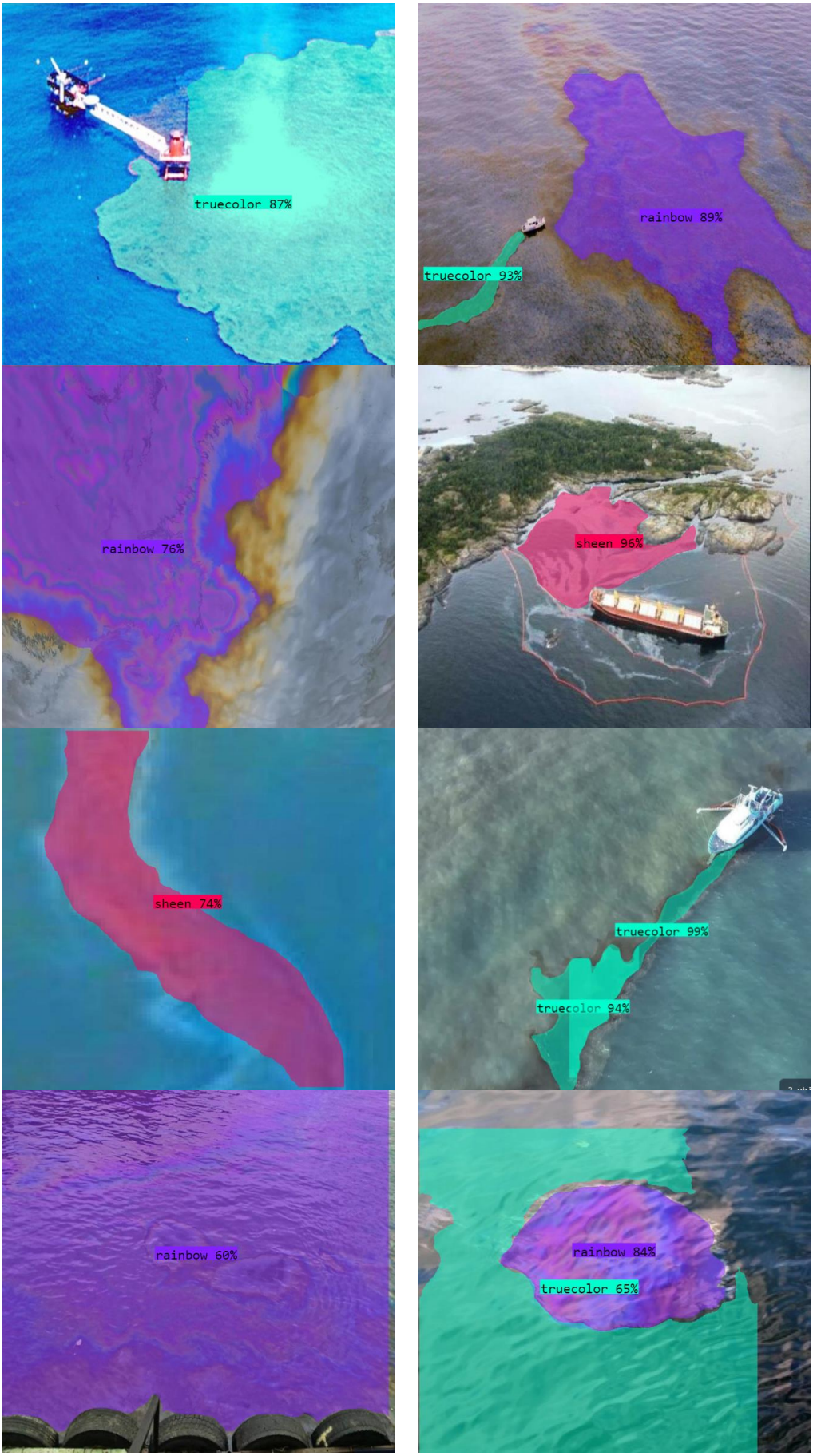
truecolor 87%
rainbow 89%
truecolor 93%
rainbow 76%
sheen 96%
sheen 74%
truecolor 99%
truecolor 94%
rainbow 60%
rainbow 84%
truecolor 65%

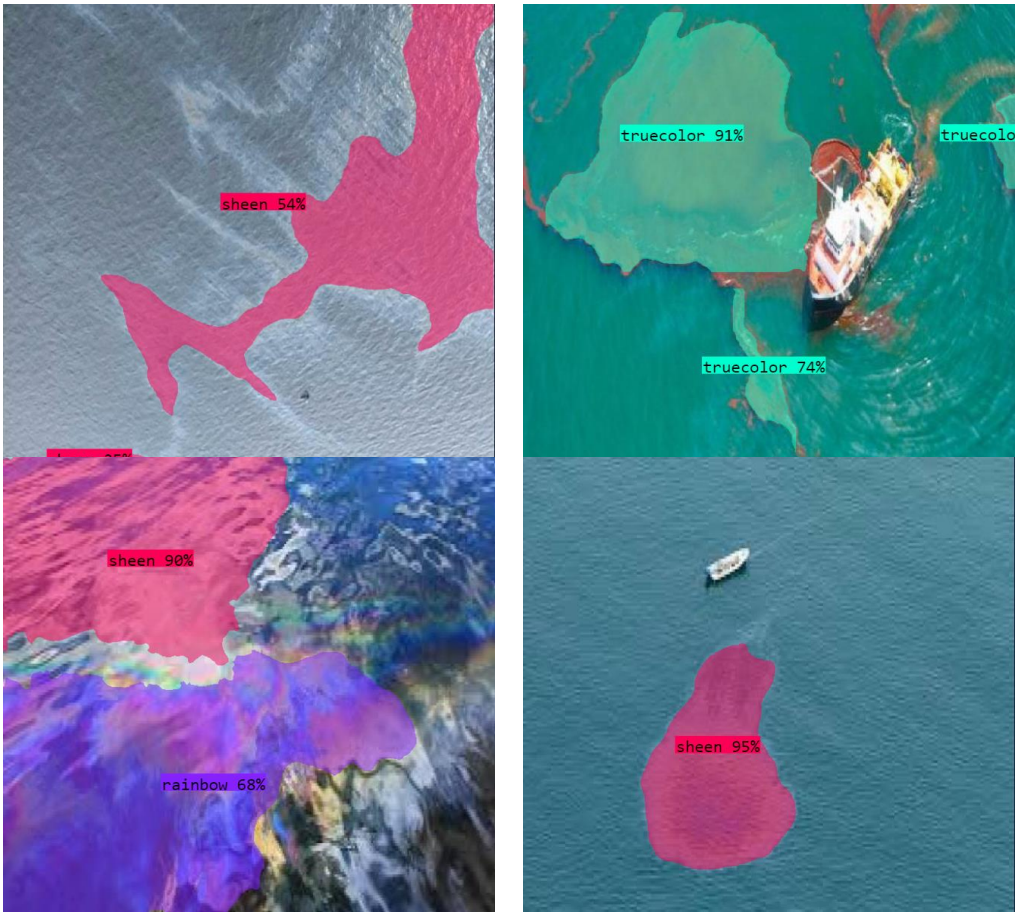

Figure 6. Oil Spill segmentation on test data (detecting oil thickness level by classifying between 'rainbow', 'sheen' and 'truecolor' classes)**.**

The segmentation appears to be reasonably accurate in most areas, capturing the majority of the oil spills. The images on Figure 6 showcase the results of instance segmentation applied to detecting oil spills and classifying their thickness levels using the Bonn Agreement Oil Appearance Code (BAOAC) [23,24]. The different classes indicate the oil spill thickness, which is categorized into types such as "rainbow", "sheen", and "truecolor", each representing a specific thickness level based on visual appearance. The purple areas with labels such as "rainbow 76%" or "rainbow 60%" depict thin oil films on water. The rainbow effect occurs due to light interference on the thin oil layer. The red-colored regions marked as "sheen 96%" or "sheen 74%" refer to very thin layers of oil that appear transparent or with minimal color. The high percentage indicates the model's confidence in identifying this class. The predicted green areas, such as "truecolor 99%" or "truecolor 94%", represent thicker oil layers where the oil color dominates, typically seen in spills where the oil forms a more opaque film.

The predicted results provide an estimation of the oil spill's thickness. These segmentations assist in analyzing the distribution of different thickness levels of oil spill across the water surface.

5. Conclusions

This study contributes significantly to environmental monitoring by leveraging instance-based segmentation for the accurate detection and segmentation of oil spills using drone footage. The proposed system integrates advanced computer vision models to estimate oil spill characteristics, such as thickness, which is crucial for effective decision-making in cleanup operations. With a mAP of 91%, the model demonstrates its effectiveness in real-time monitoring, enabling quick and efficient responses to environmental hazards.

Future research could focus on refining the model's accuracy across varying environmental conditions and expanding its applicability to detect a broader range of spill types and area, thereby enhancing the overall impact of oil spill response efforts.

Author Contributions: T.M. designed methodology. designed and developed the system and ML model. P.M. conceptualized the idea for this manuscript. supervised and administered the work. prepared the original draft. validated the data and results. S.T. carried out the investigation and data curation of the acquired data. validated the data and results. All authors have read and agreed to the published version of the manuscript.

Funding: This research received no external funding.

Institutional Review Board Statement: Not applicable.

Informed Consent Statement: Not applicable.

Data Availability Statement: The data presented in this study are available on request from the first author.

Conflicts of Interest: The authors declare no conflicts of interest.

References

1. Michel, J.; Fingas, M. Oil Spills: Causes, consequences, prevention, and countermeasures. In *Fossil Fuels: Current Status and Future Directions*; 2016; pp. 159–201.
2. Kingston, P.F. Long-term environmental impact of oil spills. *Spill Sci. Technol. Bull.* **2002**, *7*, 53–61.
3. Beyer, J.; Trannum, H.C.; Bakke, T.; Hodson, P.V.; Collier, T.K. Environmental effects of the Deepwater Horizon oil spill: A review. *Mar. Pollut. Bull.* **2016**, *110*, 28–51.
4. Bayramov, E.; Kada, M.; Buchroithner, M. Monitoring oil spill hotspots, contamination probability modelling and assessment of coastal impacts in the Caspian Sea using SENTINEL-1, LANDSAT-8, RADARSAT, ENVISAT and ERS satellite sensors. *J. Oper. Oceanogr.* **2018**, *11*, 27–43. https://doi.org/10.1080/1755876X.2018.1438343.
5. Rajendran, S.; Vethamony, P.; Sadooni, F.N.; Al-Kuwari HA, S.; Al-Khayat, J.A.; Seegobin, V.O.; Nasir, S. Detection of Wakashio oil spill off Mauritius using Sentinel-1 and 2 data: Capability of sensors, image transformation methods and mapping. *Environ. Pollut.* **2021**, *274*, 116618.
6. Bayramov, E.; Buchroithner, M. Modelling of oil spill frequency, leak sources and contamination probability in the Caspian Sea using multi-temporal SAR images 2006–2010 and stochastic modelling. *Geomat. Nat. Hazards Risk* **2015**, *7*, 1175–1197. https://doi.org/10.1080/19475705.2015.1007536.
7. Chen, Y.; Wang, Z. Marine oil spill detection from SAR images based on attention U-Net model using polarimetric and wind speed information. *Int. J. Environ. Res. Public Health* **2022**, *19*, 12315.
8. De Kerf, T.; Gladines, J.; Sels, S.; Vanlanduit, S. Oil spill detection using machine learning and infrared images. *Remote Sens.* **2020**, *12*, 4090.
9. Topouzelis, K.N. Oil spill detection by SAR images: Dark formation detection, feature extraction and classification algorithms. *Sensors* **2008**, *8*, 6642–6659.
10. Fiscella, B.; Giancaspro, A.; Nirchio, F.; Pavese, P.; Trivero, P. Oil spill detection using marine SAR images. *Int. J. Remote Sens.* **2000**, *21*, 3561–3566.
11. De Kerf, T.; Gladines, J.; Sels, S.; Vanlanduit, S. Oil spill detection using machine learning and infrared images. *Remote Sens.* **2020**, *12*, 4090.
12. Koirala, B.; Mboga, N.; Moelans, R.; Knaeps, E.; Sels, S.; Winters, F.; ; Scheunders, P. Study on the Potential of Oil Spill Monitoring in a Port Environment Using Optical Reflectance. *Remote Sens.* **2023**, *15*, 4950.
13. Otremba, Z.; Piskozub, J. The modification of light flux leaving a wind-roughened, oil covered sea surface example of computations for shallow seas. *Ocean. Stud.* **2000**, *29*, 117–133.
14. Otremba, Z. A thin oil film covering the sea surface as a modifier of the downward transmission of light. *Oceanologia* **1997**, *39*, 397–411.
15. Fingas, M. Visual appearance of oil on the sea. *J. Mar. Sci. Eng.* **2021**, *9*, 97.
16. Megan Ewald. How Thick is the Oil Spill? 2020. Available online: https://blog.response.restoration.noaa.gov/index.php/how-thick-oil-spill (accessed on).
17. Fingas, M.F.; Brown, C.E.; Gamble, L. The Visibility and Detectability of Oil Spills and Oil Discharges on Water. In Proceedings of the Twenty-Second Arctic and Marine Oil Spill Program Technical Seminar, Environment Canada, Ottawa, ON, Canada, 2–4 June 1999; pp. 865–886.
18. Hornstein, B. *The Appearance and Visibility of Thin Oil Films on Water, Environmental Agency Protection Report*; EPA-R2-72-039; US Environmental Protection Agency: Cincinnati, OH, Canada, 1972.

19. Hornstein, B. The Visibility of Oil-Water Discharges. In Proceedings of the 1973 International Oil Spill Conference, Washington, DC, USA, 13–15 March 1973; American Petroleum Institute: Washington, DC, USA, 1973; pp. 91–99.
20. Bayramov, E.; Kada, M.; Buchroithner, M. Monitoring oil spill hotspots, contamination probability modelling and assessment of coastal impacts in the Caspian Sea using SENTINEL-1, LANDSAT-8, RADARSAT, ENVISAT and ERS satellite sensors. *J. Oper. Oceanogr.* **2018**, *11*, 27–43. https://doi.org/10.1080/1755876X.2018.1438343.
21. COCO Dataset. Available online: https://github.com/ultralytics/ultralytics/blob/main/ultralytics/cfg/datasets/coco.yaml (accessed on).
22. YOLOv8 Segmentation Models. Available online: https://docs.ultralytics.com/tasks/segment/ (accessed on).
23. BA Color Codes and Oil Volume Estimation. Available online: https://odnature.naturalsciences.be/mumm/en/national/ba-oil-appearance-code (accessed on).
24. Agreement, B. *Bonn Agreement Oil Appearance Code—Photo Atlas*; Version 23/06/2011; Bonn Agreement, London, UK, 2011.